Skin Friction Measurements using Oil Film Interferometry and Laser Doppler Anemometry

T. Gunnar Johansson,[*] Faraz Mehdi,[†] Farzad Shiri,[‡]
Chalmers University of Technology, SE-41296 Göteborg, Sweden

and

Jonathan W. Naughton[§]
University of Wyoming, Laramie, WY, 82071

The measurement of wall shear stress using three techniques that are exact in principle have been carried out in a wall jet. The purpose of these measurements is to compare the results of these three methods to assess their capabilities and shortcomings since accurate wall shear stress measurements are important for both fundamental studies and applications such as viscous drag reduction. Oil film interferometry (OFI) and laser Doppler anemometry (LDA) measurements have been carried out at several locations downstream of the wall jet exit. Velocity profiles from the LDA measurements have been analyzed using a wall-gradient method and a momentum-integral approach. The theory behind each of these approaches is briefly described. The oil film method produces reasonable results at all conditions tested although the scatter was higher than desired. The wall gradient method yielded results consistent with the OFI results at low velocities and distances far from the jet exit where the near-wall velocity profile was well-resolved. The momentum integral approach compared poorly to the other methods, a result that we believe is due to terms in the momentum integral that were not measured.

Nomenclature

b	=	jet exit height
c	=	perspective center
C_f	=	skin friction coefficient
h	=	height of the oil
n	=	streamline divergence
$\hat{n}$	=	surface normal
n_f	=	oil index of refraction
n_a	=	air index of refraction
q	=	dynamic pressure
Re	=	Reynolds number
t	=	time
$\overline{U}, \overline{V}$	=	mean velocities in x- and y-directions
U_0	=	jet exit velocity
$\overline{u^2}, \overline{v^2}$	=	normal Reynolds stresses

[*] Associate Professor, Department of Applied Mechanics, AIAA Senior Member.
[†] M. Sc. student, Department of Applied Mechanics.
[‡] Ph.D. student, Department of Applied Mechanics.
[§] Associate Professor, Department of Mechanical Engineering, Dept. 3295, 1000 E. University Avenue, AIAA Associate Fellow.

$\overline{uv}$ = Reynolds shear stress
u_τ = friction velocity
x,y,z = Cartesian coordinates
X,Y = Cartesian coordinates – image space

θ = angle between line through perspective center and surface normal
θ_i = incidence angle
λ = wavelength
μ = dynamic viscosity
ν = kinematic viscosity
ρ = density
τ_w = wall shear stress
ϕ = phase

I. Introduction

Wall shear stress or skin friction continues to be a difficult quantity to measure with good accuracy. This shortcoming is important because skin friction is fundamental to both basic fluid physics (e.g. scaling of wall bounded turbulent flows) as well as practical applications (e.g. determination of friction drag on vehicles). Even after 100 years of investigation, it is disappointing that wall shear stress measurements are often missing from such studies, or, if they are made, uncertainties on the order of 20% are deemed acceptable.

Over the past several years, the uncertainty of two techniques suitable for measuring mean wall shear stress, velocity profiles via Laser Doppler Anemometry (LDA) and Oil Film Interferometry (OFI), has been shown to be quite low provided that the measurements and analysis are done with great care. The present work considers the use of both LDA and OFI in a two-dimensional wall jet to compare the respective wall shear stress measurements.

There are at least two methods available to determine the wall shear stress in turbulent wall bounded flows from measurements of the velocity field: the determination of the mean velocity gradient at the wall, and the integration of the momentum equation. Both methods are characterized by not requiring any assumptions about the functional form of the velocity profile or knowledge of any other flow properties, and are, in this sense, exact methods. This statement also holds true for the oil film interferometry method.

In spite of the theoretical advantages of the velocity-profile methods, their accuracy is often in question. The wall gradient method requires very precise measurements of the velocity field very close to the wall, measurements that are often very difficult to obtain. The momentum integral method, in most cases, requires that more than just the mean momentum terms are included, especially the pressure term and the Reynolds stresses. More significantly, though, the measurements must be very precise to permit accurate spatial derivatives in the slowly varying mean flow direction to be determined. Such measurements are extremely time consuming.

Johansson and Castillo (2002) demonstrated that both velocity-profile methods could be made to work satisfactorily in a low Reynolds number flat plate experiment using laser Doppler anemometry. However, it was clear that the measurement of mean velocity in the extreme vicinity of the wall was contaminated by some agent causing the measured mean velocity to be too high at locations close to the wall. It was also clear that there were difficulties with the momentum integral method. In particular, it became evident that an unexpectedly high spatial resolution was necessary in the outer part of the boundary layer, and, even for the nominally zero pressure gradient boundary layer studied, the very small pressure gradient term could not be neglected. These findings partly motivated the present investigation.

In recent years, significant improvements have been made to the oil film interferometry method. This method has several advantages. Like the previously mentioned methods, it is exact, but, in contrast to these methods, it is less time consuming, it simultaneously provides data at many locations on a surface, and, perhaps of most importance, it can be applied in high Reynolds number flows. Although the accuracy of oil-film interferometry methods has been considered in several papers, a direct comparison with a technique of equal accuracy has been missing.

In the present investigation, an initial attempt has been made to employ all three methods and to compare them. A wall jet was chosen because it was already available, it gave a significant variation in wall shear stress in the downstream direction, and it was easily assessable for both for LDA and OFI measurements. Both one component LDA velocity surveys and OFI measurements were performed at several downstream locations for three jet exit

Reynolds numbers. Although the techniques compare favorably at all locations, the level of accuracy in this first attempt fell short of that we desired for the comparison and establishing a lower limit of uncertainty for each of the techniques.

A. Previous Work

The wall gradient method as well as the momentum integral method are integral parts of the basic equations of fluid mechanics. The methods have been known for a long time, and are described in practically all textbooks on the subject. Yet, the practical utilization of the methods has often proved quite difficult, and the methods have, from time to time, been abandoned. Johansson and Castillo (2002)[1] used these velocity-profile methods in a study of turbulent boundary layers on flat plates, and found that, if the velocity measurements are done with great care, sufficient spatial resolution is maintained, and all terms in the equations are taken into account, both methods work quite well for low Reynolds number boundary layers.

Image-based oil film interferometry was originally pioneered by Tanner's group in the UK during the 1970s.[2] It has subsequently been improved by Monson et al.,[3] Mateer et al.,[4] Garrison and Ackman,[5] and Naughton and Brown[6] among others. A complete summary of oil-film interferometry may be found in the recent review article by Naughton and Sheplak.[7] Although the basis of the technique has not changed, the advent of digital cameras and the processing power of micro-computers has allowed the technique to evolve substantially. Today, the combination of multiple images, calibrated oils, rigorous spatial calibration of the cameras, and sophisticated processing of the results have made it feasible to obtain highly accurate results under controlled testing conditions. The work here strives to leverage these improvements in the technique to obtain results with the maximum accuracy possible.

II. Experimental Procedure

A. Wall Jet

The experiment was carried out in a wall jet facility available in the Fluid Dynamics laboratory at Chalmers University. A schematic of the rig is shown in figure 1 (Also see figure 2). The wall jet develops along the bottom of the rig, and side walls are inserted to help maintain a two-dimensional flow. The top of the rig is open. The wall jet is 3.2 meters long, 0.985 meter wide, and 0.66 meter high. The slot is 10 mm high and 540 mm wide. Air driven by a fan passes through a converging nozzle and enters parallel to the bottom wall of the facility. The jet emanating from the nozzle has a nearly top hat mean velocity profile and a turbulence intensity of about 0.3%. The entire rig is enclosed in a plastic tent to isolate the wall jet from disturbances from the ventilation system in the laboratory and to keep the seeding used for the LDA measurements re-circulating. In order to provide a suitable background for the oil film interferometry, a strip of Mylar was attached to the bottom surface of the rig. This strip was also in place during the LDA measurements to make sure that the flow conditions were the same. The width of the Mylar sheet is 125 mm. A high-precision traverse system was placed below and to the side of the rig to accomplish the traverse of the LDA probe volume.

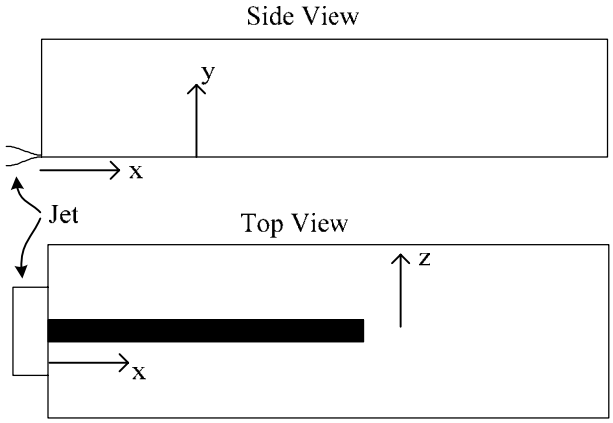

Figure 1 - Schematic of the wall-jet rig.

B. Laser Doppler Anemometry

A one-component Dantec fiberoptic LDA system was used for the velocity measurements. A 1200 mm focusing beam expander (expansion ratio 1.55) and two parallel expanders with an expansion ratio of 1.94 each were used to reduce the probe volume size to 60 μm in diameter and about 1.2 mm long. The probe was mounted on a stable frame of aluminum beams and was attached to the traverse system. With this system, the probe position could be varied in all three spatial directions with a resolution of 2 μm. The setup of the LDA system is shown in figure 2.

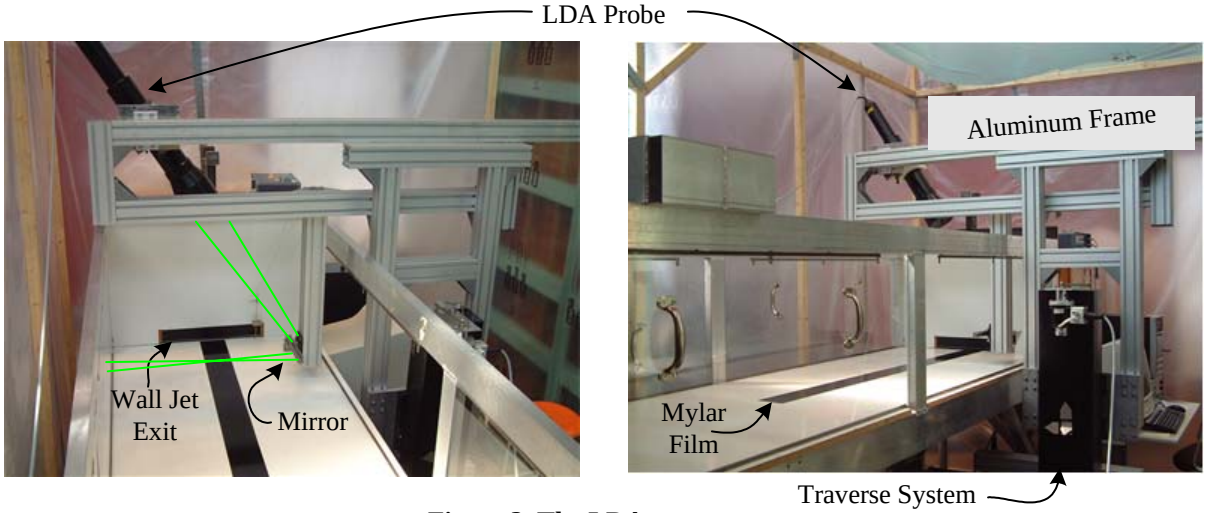

Figure 2. The LDA system set-up.

The probe was mounted well above the wall jet flow to avoid disturbances as shown in figure 2. The laser beams were redirected by a mirror to make the beams nearly parallel to the bottom wall of the channel. Finding the position of the wall in the coordinate system of the probe volume is always a difficult task. Many times it can be accomplished by positioning the probe volume close to the wall, traversing in small steps normal to the wall, and observing the signal on an oscilloscope. If the surface has suitable properties, it will scatter the laser light from the surface, and the zero position will be determined as the one that gives the largest signal amplitude. When this method works, it gives the zero position with an uncertainty of only 10-20 μm. This method worked in several of the investigated positions on the Mylar surface, but unfortunately not at all points. In some points, we had to rely on the much less accurate method of looking for the position where the laser spots on the surface appeared to merge to one point. Neither of these methods is sufficient to locate the wall with sufficient precision for determining the velocity gradient a the wall. Processing of the LDA signals was done using a Dantec N5711 BSA processor and the BSA Flow software.

C. Oil Film Interferometry

Oil film interferometry is based on the change of thickness of a thin oil film when subject to aerodynamic shear. The simplified one-dimensional form of the equation governing the motion of the thin oil film is

$$\frac{\partial h}{\partial t} + \frac{\partial}{\partial x}\left(\frac{\tau_w h^2}{2\mu}\right) = 0\,. \tag{1}$$

The thin-oil-film equation was originally derived by Squire,[8] and a complete derivation of the equation can be found in Brown and Naughton, [9] while a brief summary is presented by Naughton and Sheplak.[7] As is evident from the equation, if the height of the oil can be measured as a function of time and space, the shear stress is assumed to be only a function of space, and the viscosity of the oil is known, this equation may be used to determine the wall shear stress.

To determine the thickness of the oil, inerferometry was first suggested by Tanner's group.[2] A description of thin-film interferometry can be found in several of the references provided, and only a brief description is given here. Light illuminating the oil film partially reflects from and partially transmits through the oil. At the oil/Mylar interface, a portion of the light is reflected and returns back through the oil. When these two beams are recombined by a lens, they produce an interference pattern depending on the phase difference between the light reflected from the oil surface and that reflected from the Mylar surface. The relationship between the phase difference ϕ and the oil thickness h is given by

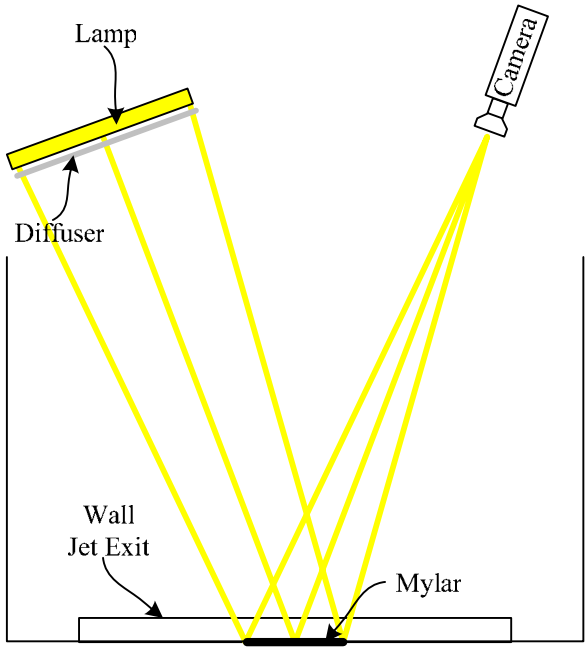

Figure 3 – Schematic of oil-film interferometry system used in the present study. The view is looking toward the exit of the wall jet.

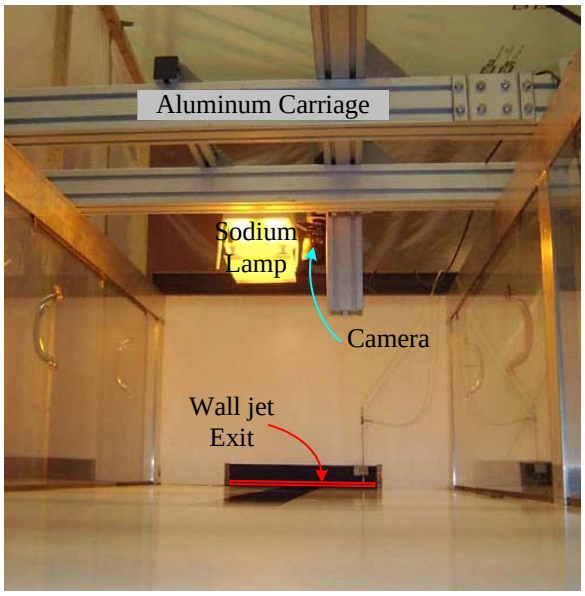

Figure 4 – Image of oil-film interferometry system installed above wall jet.

$$h = \frac{\lambda\phi}{4\pi}\frac{1}{\sqrt{n_f^2 - n_a^2 \sin^2\theta_i}}. \tag{2}$$

A schematic of the oil film interferometry system used in this experiment is shown in figure 3 and an image is shown in figure 4. A sodium lamp with two closely spaced emission lines 589.0 and 589.6 nm was used to illuminate the oil films. The oil films were created by applying a film of Dow Corning 200 Fluid to a Mylar film attached to the surface of the wall jet and exposing the thin film to the wall jet. Images of the film were captured throughout a test using a Kodak MegaPlus ES 1.0 CCD camera with a spatial resolution of 1008 x 1018 and an interpixel spacing of 9 microns. The camera was computer controlled using Dantec's Flowmaster PIV Software. A Nikon 60 mm focal length lens was selected to image the interferograms taken here. The lamp and camera were mounted on an overhead traverse that could be located at different distances from the wall jet exit.

Critical to the accuracy of the wall shear stress measurements obtained via OFI is an accurate calibration of the oil viscosity. The viscosity of the 20, 50, and 100 cs Dow corning 200® fluids used in this experiment were calibrated at SP Swedish National Testing and Research Institute to determine their behavior with temperature. Exponential fits to the data were performed, and the resulting fits were used to calculate the oil viscosity as the temperature varied during a run.

During a test, specific steps were followed to ensure that the data necessary for analyzing the oil film data were available. First, an image of the illuminated Mylar surface is taken to determine the mean intensity variations in the images. Next, a grid containing a set of known points was laid on the surface at a known location and an image was taken. As explained below, this image is necessary to determine the location of the camera in model space. Next, oil was applied to the surface using a straight edge that, when drawn along the surface, produced a rather "thick" oil film. At this point, the data acquisition program that monitored the test conditions as well as triggered the camera to snap images was started. Typical separation times were 4-30 seconds depending on the test case and oil viscosity. At the end of a run, the wall jet was shut down and the data acquisition process was terminated. Both interferograms and test conditions are saved for later analysis.

III. Determination of Wall Shear Stress

A. Test Cases

In order to provide multiple comparisons of the predicted wall shear stress values, measurements were made for several different conditions. Using the LDA measurements, near wall fits and/or the momentum integral was used to determine the wall shear stress at multiple downstream locations for three velocities. Oil film measurements were made at the same downstream locations for three velocities using three different viscosities. All of the test cases are summarized in Table 1.

Table 1 – Test cases for the present study; VG – velocity gradient, MI – momentum integral, and OFI – oil film interferometry.

Speed	Distance from slot						
m/s	0.25 m	0.50 m	0.75 m	1.00 m	1.25 m	1.50 m	1.60 m
20	VG	OFI VG MI	VG MI	OFI VG MI	VG MI	OFI VG MI	VG
40		OFI VG		OFI VG MI		OFI VG	
54		OFI VG		OFI VG MI		OFI VG	

B. Velocity Profile

The wall shear stress can be determined from velocity measurements in at least two different ways, using the gradient at the wall, and from an integration of the momentum equations (Johansson and Castillo, 2002). Both of these methods are exact in the sense that they do not require any assumptions to be made about the functional form of the profile, or any knowledge about any other property of the flow field. Therefore, if careful measurements are carried out, it should be possible to determine the wall shear stress accurately using these methods.

These methods both go back to a straightforward integration of the momentum equation

$$\int_0^y \frac{\partial \overline{U}^2}{\partial x} dy' + \int_0^y \frac{\partial \overline{UV}}{\partial y} dy' = \int_0^y \frac{\partial \overline{v^2}}{\partial x} dy' + \nu \int_0^y \frac{\partial^2 \overline{U}}{\partial y^2} dy' - \int_0^y \frac{\partial \overline{u^2}}{\partial x} dy' - \int_0^y \frac{\partial \overline{uv}}{\partial y} dy' . \tag{3}$$

Note that we have neglected all possible effects of three-dimensionality. In a wall jet, the mean free-stream pressure term is exactly zero, but the pressure variation within the wall jet due to the wall-normal Reynolds's stress $\overline{v^2}$ still needs to be included. With the aid of the continuity equation, this equation can directly be integrated to

$$\frac{\tau_w}{\rho} = \overline{U} \int_0^y \frac{\partial \overline{U}}{\partial x} dy' - \int_0^y \frac{\partial \overline{U}^2}{\partial x} dy' + \nu \frac{\partial \overline{U}}{\partial y} - \int_0^y \frac{\partial \overline{u^2}}{\partial x} dy' + \int_0^y \frac{\partial \overline{v^2}}{\partial x} dy' - \overline{uv} . \tag{4}$$

For $y \to 0$, we obtain

$$\frac{\tau_w}{\rho} = \nu \left. \frac{\partial \overline{U}}{\partial y} \right|_w , \tag{5}$$

which is the wall gradient method. For $y \to \infty$, we obtain

$$\frac{\tau_w}{\rho} - = -\int_0^\infty \frac{\partial \overline{U}^2}{\partial x} dy' - \int_0^\infty \frac{\partial \overline{u^2}}{\partial x} dy' + \int_0^\infty \frac{\partial \overline{v^2}}{\partial x} dy \,, \tag{6}$$

which is a momentum integral method. We thus see that, by either carrying out an accurate set of measurements very near the wall or carrying out accurate measurements throughout the wall jet, we can obtain the wall shear stress. With a one-component system, the last term in equation (6) cannot be measured. This is a severe drawback, since this term cannot be neglected in a wall-jet. The momentum integral method requires that the full profiles are measured in several not too distant positions. In principle, the profiles can be truncated at an arbitrary distance from the wall, but, in such a case, we would of course also have to measure the $\overline{uv}$ correlation, as is evident from equation (4).

As can be easily demonstrated, the mean velocity profile very near the wall can be written as

$$\overline{U} = \frac{\tau_w}{\mu} y + \left. \frac{\partial^4 \overline{U}}{\partial y^4} \right|_w y^4 + O\left(y^5\right). \tag{7}$$

By careful measurements of the mean velocity profile very near the wall, the wall shear stress can be determined by a fit to the functional form expressed in equation (7).

Once the wall shear stress is obtained, the friction velocity

$$u_\tau = \sqrt{\frac{\tau_w}{\rho}} \tag{8}$$

and the skin friction coefficient

$$c_f = \frac{\tau_w}{\frac{\rho}{2} U_s^2} \tag{9}$$

can be determined. Here, we have chosen to base the skin friction coefficient on the slot velocity U_s.

C. Oil Film Interferograms

The determination of wall shear stress from oil film interferograms is discussed in several references (see Naughton and Sheplak[7] and Naughton et al.[10] for example), but it will be briefly discussed here. The analysis consists of several discrete steps, all of which are presented here.

1. Camera Calibration

The first step necessary in quantitative visualization for any purpose is the calibration of the imaging device. The process of calibrating the camera in this study follows the photogrammatic methods outlined by Cattafesta and Moore[11] or Liu et al. [12] Here we will only briefly describe the process as an in-depth paper on the subject is currently in preparation.

Photogrammetry is the process of mapping image space into model space and vice-versa. Figure 5 shows the relationship between camera space and model space. All points in model space arrive at the image plane of the camera through the principal point (x_c,y_c,z_c). Here, the image space is given by coordinates X, Y, and the model space is a separate coordinate system given by x, y, z. The intent of photogrammetry is to map every point on the model into image space. To accomplish this, two sets of parameters, the internal and external orientation parameters, are required. The internal orientation parameters are characteristic of the lens/camera system whereas the external orientation parameters describe the location of the camera in model space and are specific to the region of the model being imaged.

For a model with strong three-dimensionality, the internal and external orientation parameters can be determined in a single step. In this study, the surface being imaged is two-dimensional, so this approach is not possible.

Instead, the interior orientation points are first determined using a three-dimensional step model, and then the external orientation parameters are determined from reference points on the model that are taken just before a run.

Using the interior and exterior orientation parameters, the mapping between image space and model space is possible. The angle between the surface normal $\hat{n}$ and a line passing through the perspective center to the point may also be determined and is equal to the incidence angle of the light striking the surface of the oil film. With the location on the model and the angle of incidence, all of the information needed to determine the oil height is available.

2. Image Analysis-Determination of Oil Thickness

As evident from the oil-film equation, the interferograms obtained during a run are first converted to height before the shear stress may be determined. From the series of images acquired during a test, one is chosen for analysis. Since the flow here is two-dimensional, lines parallel to the flow direction are analyzed. The locations are chosen in physical space, and appropriate lines are extracted from the interferogram. The minima and maxima of intensity in each of these lines are extracted from the lines using the method discussed by Decker (see Decker et al.[13] and Naughton et al.[10] for details). Figure 6 (a) shows the locations of the maxima and minima in the fringe pattern that have been identified for each of the lines analyzed. The points nearest to the leading edge are used to determine the leading edge location using extrapolation. Since the phase is known at each of the locations identified in figure 6(a), the height may be calculated using equation xx, the oil properties, and the light incidence angle available from the photogrammetry results. The height distribution for the image in figure 6 (a) is shown in Figure 6 (b).

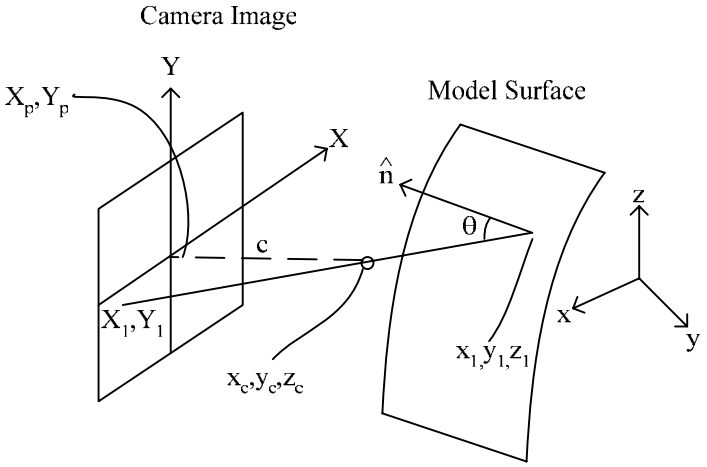

Figure 5 – Schematic of model space and image space and the important parameters associated with them.

3. Determination of Skin Friction

Once the thickness of the oil film is known, only the solution of Equation (1) is required. Several approaches have been used, but here we use the iterative approach of Garrison and Ackman.[5] In this approach, the skin friction is determined using

$$C_{f,i+1}^{1/2} = \frac{\int_0^x (n/C_{f,i})^{1/2} dx}{hn^{1/2} \int_0^t \frac{q}{\mu} dt}. \tag{10}$$

This iterative solution requires an initial guess that is provided by the constant wall shear stress solution

$$C_{f,1} = \frac{\mu x}{qht} \tag{11}$$

The streamline divergence n here is 1 since the flow is two-dimensional, and the integral in the denominator is determined from the flow conditions monitored during the test. The solution converges to an acceptable level in just a few iterations. The skin friction values determined from the interferogram in figure 6(a) are shown in figure 7 where both the individual values in figure 7(a) and values averaged across z and over a range of x in figure 7(b) are given.

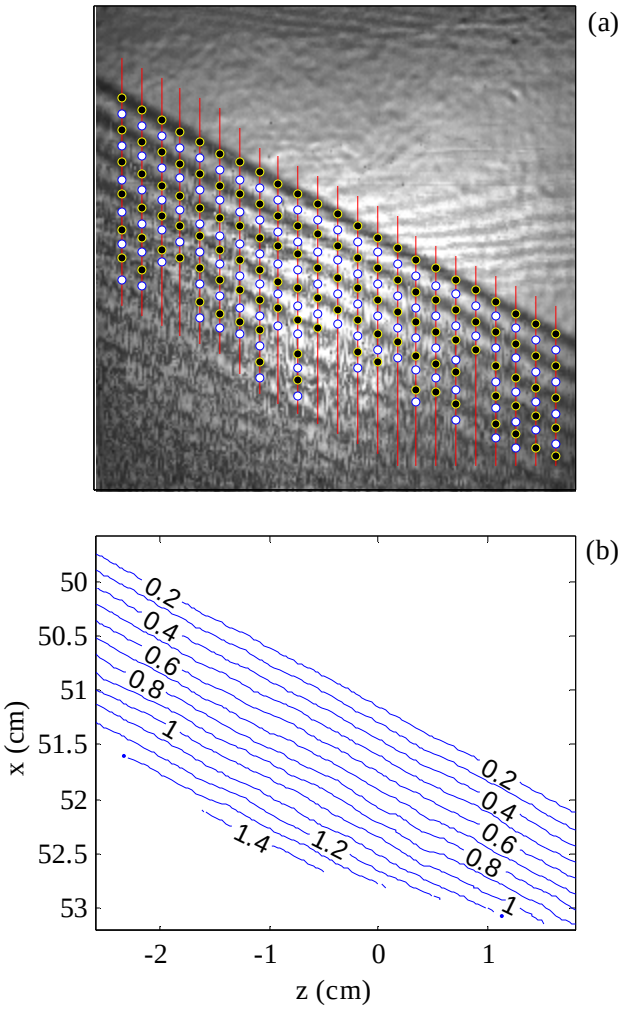

Figure 6 – Height determined from interferogram: (a) interferogram with analysis lines and intensity maxima and minima identified, and (b) contours of the oil-film thickness.

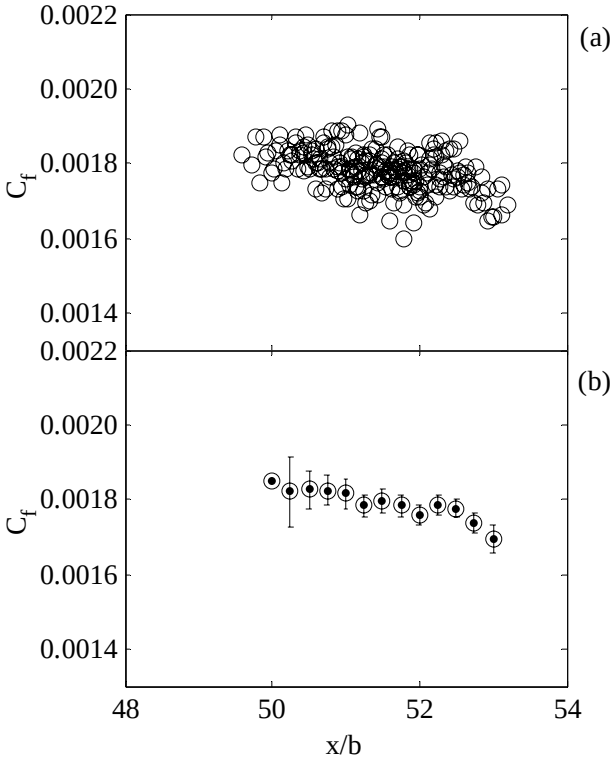

Figure 7 – Skin friction data for U_0=54 m/s and x/b=50 case: (a) all 233 data points determined from interferogram and (b) averaged over a range of x.

IV. Results and Discussion

A. Velocity field measurements

1. Wall gradient method

An example of a mean velocity profile near the wall is shown in figure 8(a). From this figure it is immediately clear that the points closest to the wall must be wrong. This is an effect that has also been observed by others, for example Johansson and Castillo,[1] and Karlsson and Eriksson.[14] To cope with this problem the profiles are inspected, and the innermost points are removed from the fitting procedure. Another problem that occurs is that, if too many points are included in the fit, the fourth order polynomial used is no longer appropriate, and the number of included points must be truncated. This is done by visual inspection of the fits using different number of points. Fortunately, the wall shear stress is not highly sensitive to the exact truncation point as long as it is reasonable. Unfortunately, the useful range of near-wall points decreases rapidly with increasing wall shear stress, and, in the case of high shear stress, this approach becomes less accurate.

We also notice that the fitted curve does not cross the y-axes at the origin. This is caused by the difficulty of determining the position of the probe volume in relation to the wall. The "error" is in this particular case about 40 μm, a little more than half the diameter of the diameter of the probe volume.

It is noted that the mean velocity values closest to the wall show an apparent increase. This is believed to be a bias effect due to a systematic rejection of low speed samples. Very close to the wall the probe volume spans a normal distance over which the mean velocity may vary by a factor of two or more. Since there is a larger volume of fluid flowing through the outer part of the probe volume than through the inner part, there is an increased risk that during the passage time of a low speed particle close to the wall, also a high speed particle may cross in the outer part. When this happens the Doppler signal is significantly distorted, and the validation process built into the BSA processors is likely to reject the sample. In principle it should be possible to test this hypothesis by systematically varying the seeding level, but this has unfortunately not yet been done due to the limited measuring time available.

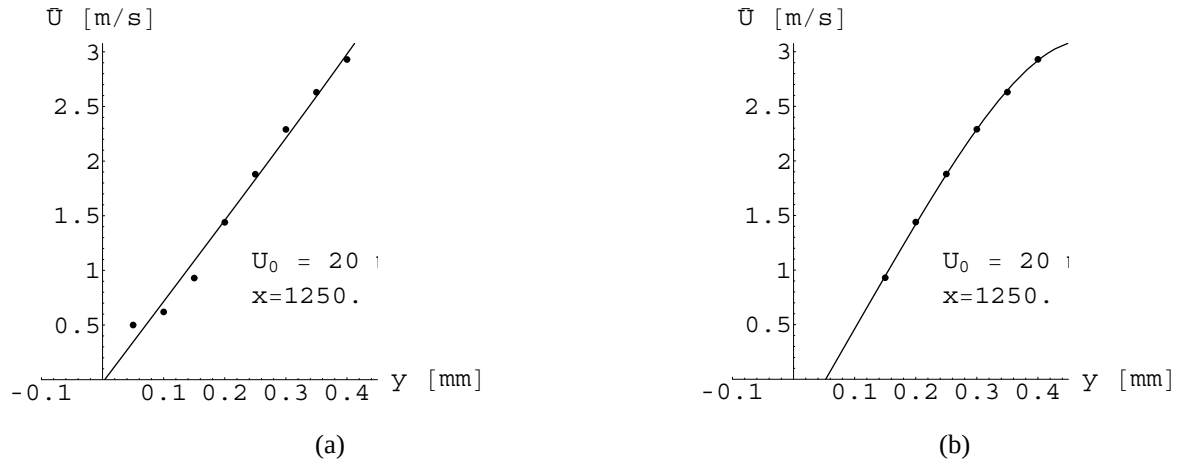

(a) (b)

Figure 8 - Near-wall velocity profile, and estimated fitting polynomial: (a) all near-wall points fit, and (b) two points nearest the wall removed.

The variation in c_f along the wall for the slot outlet speed of 20 m/s is shown in figure 9. As expected the skin friction coefficient decreases monotonically with increasing distance from the slot. As will be demonstrated later this is in general agreement with the oil film data.

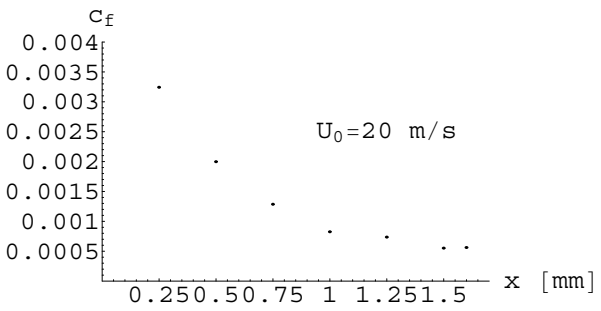

Figure 9 - The variation in skin friction coefficient along the wall for the slot outlet speed of 20 m/s. The wall gradient method was used.

2. Momentum integral method

In order to evaluate the wall shear stress using the full momentum integral, the mean velocity profiles and the normal Reynolds' stresses profiles are needed, equations (4) and (6). In this experiment it was regretfully not possible to measure the wall-normal stress due to a malfunction of some of the fiber couplers in the LDA system. For the same reason, neither could the Reynolds shear stress be measured. It must be emphasized that these terms are quite important for the momentum balance to work properly.

Figure 10 shows the profiles of mean velocity, rms velocity, and the squares of these quantities, which are the quantities actually used in the momentum balance. These profiles have the expected general shape. The mean velocity increases from zero at the wall, reaches a maximum value at a fairly short distance from the surface, and then decays back to zero. The rms profile shows a more complex behaviour. There are two peaks, one very close to the wall, and one farther away from the wall. Outside of the second peak the rms values decreases to a value close to zero. It should be noted that the rms profile attains larger values than the mean velocity in the outer part of the wall jet, implying that the exchange of momentum across a vertical surface is dominated by turbulent motions in this

region of the flow field. In the larger part of the wall-jet though, the momentum exchange due to the mean velocity field dominates.

The important terms in the momentum equations (4) and (6) are however not the integrals of the squares of the mean or rms velocities, but the stream-vise derivatives of them. These derivatives can be inferred from figure 11, where a set of profiles for different stream-vise positions are shown. We notice that the peak value in the mean velocity decreases farther downstream. This is also the case for the second peak in the rms profile. The distance from the wall, where these peaks are found, increases with increasing distance from the jet exit. The thickness of the wall-jet also increases farther downstream. We realize that these contributions to the momentum integral change sign from negative to positive as we move away from the wall. Judging from these figures, it appears that the outer part of the profiles contribute the larger part of the total contribution to the momentum integral.

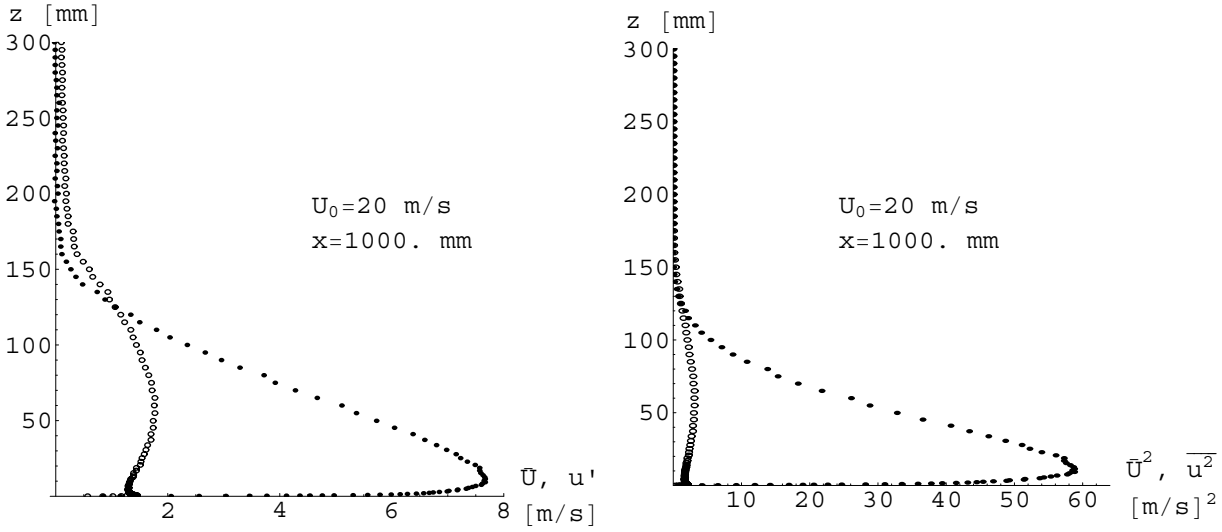

Figure 10 - Profiles of mean velocity and u', and the corresponding squared quantities used in the momentum integral method.

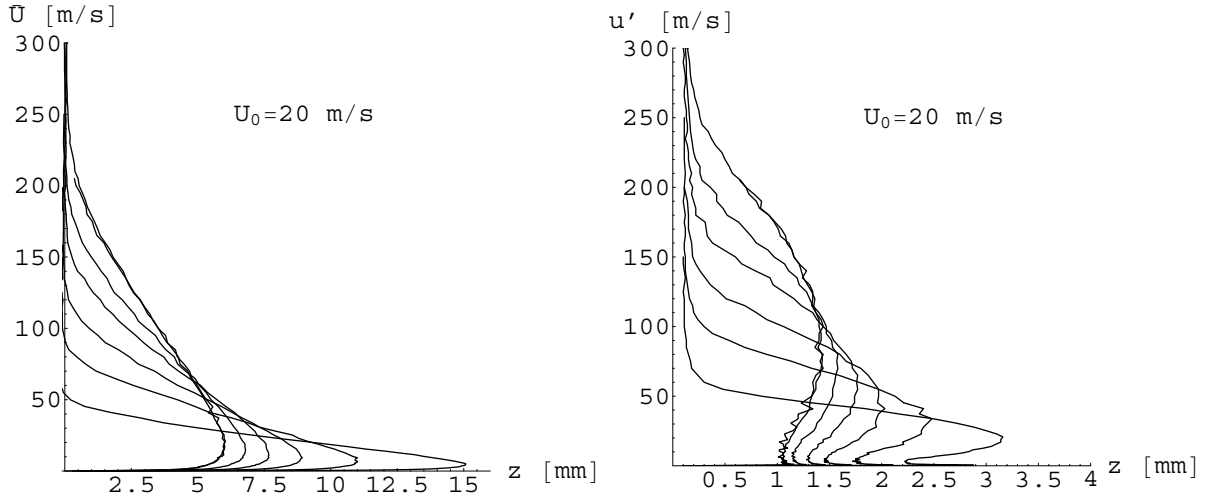

Figure 11 - The variation in mean velocity and rms fluctuations at different streamvise locations.

Unfortunately it turns out that the momentum integrals probably not are carried out far enough from the wall. Some of the terms in equation (6), which goes to zero far from the wall, probably still contributes to the integral at the distances where the measurements were stopped. The computed wall shear stresses from the momentum integral in equation (6) gives results that are quite far from the ones deduced using the wall gradient and oil film methods and are shown in figure 12. Since the momentum integral method is supposed to work for high as well as for low values of wall shear stress, this issue is worthy of further investigations.

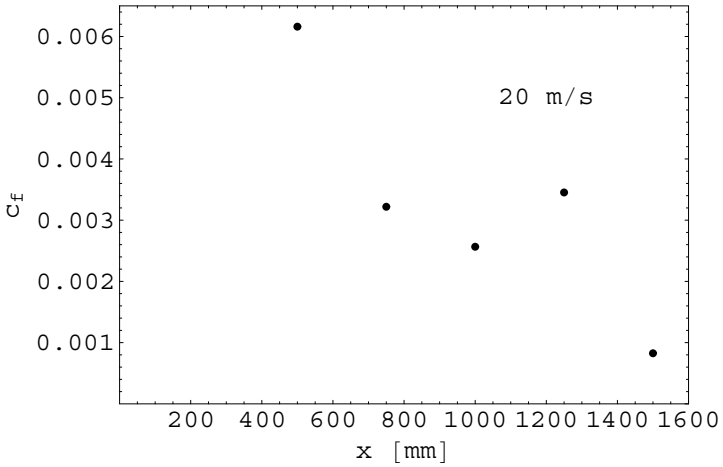

Figure 12 – Skin friction coefficient predicted by the momentum integral.

B. Oil film interferometry

The results of analyzing the interferograms as discussed above has yielded OFI results in the vicinity of x/b= 50, 100, and 150. As indicated in Table 1, the wall shear stress has been determined using OFI for three free-stream velocities. For each velocity/location combination listed in Table 1, the test has been repeated with two different viscosities. Figure 13 shows the locally-averaged skin friction values for all 18 OFI tests. As is apparent from the figure, the data are tightly clustered when plotted on a scale appropriate for the entire region covered. Different viscosities produced nearly identical results for the same test conditions. There does appear to be a slight Reynolds number dependence at x/b=50 and 100, but the values are too low and the uncertainty is too high to make any claims at x/b=150. Although these results demonstrate the capabilities of oil film interferometry when applied carefully, the current results do not have the accuracy we desired for this study. Possible causes for the uncertainties in the current test means for remedying them are presented in the next section.

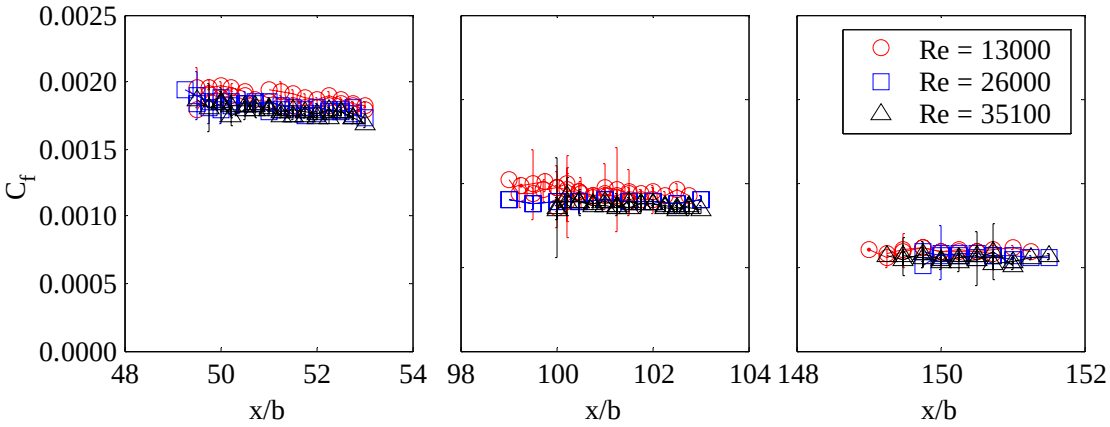

Fig 13 – Skin friction distributions at three downstream locations determined using oil-film interferometry.

C. Comparison and Summary

The previous sections have discussed the skin friction determined using velocity field measurements and oil-film interferometry. Here these measurements are summarized and compared. Figure 14 shows the friction velocity at the several different locations measured, and Table 2 summarizes the results. The oil film data are in agreement with expectations, and the scatter is low. As expected the wall shear stress decreases in the downstream direction, and

with a lowering of the jet exit speed. We note that the method seems to work equally well regardless of the wall friction level.

Table 2 – Summary of Skin Friction Results: OFI – oil film interferometry, VG – velocity gradient, and MI – momentum integral.

Speed	Distance from slot						
m/s	0.25 m	0.50 m	0.75 m	1.00 m	1.25 m	1.50 m	1.60 m
20	VG (0.00324)	OFI 20 cs (0.00189) 50 cs (0.00197) VG (0.00200) MI (0.00616)	VG (0.00129) MI (0.00322)	OFI 20 cs (0.00096) 50 cs (0.00096) VG (0.00083) MI (0.00257)	VG (0.00076) MI (0.00345)	OFI 20 cs (0.00059) 50 cs (0.00059) VG (0.00055) MI (0.00083)	LDA VG (0.00056)
40		OFI 50 cs (0.00179) 100 cs (0.00188) VG (0.00127)		OFI 20 cs (0.00088) 50 cs (0.00088) VG (0.00081) MI (0.00374)		OFI 20 cs (0.00058) 50 cs (0.00057) VG (0.00049)	
54		OFI 50 cs (0.00183) 100 cs (0.00185) VG (0.00148)		OFI 50 cs (0.00085) 100 cs (0.00084) VG (0.00069) MI (0.00413)		OFI 50 cs (0.00053) 100 cs (0.00054) VG (0.00028)	

The wall gradient method gives results that are in agreement with qualitative expectations, i.e., the wall shear stress decreases both with distance from the inlet and with a reduction of the inlet jet speed. We also notice that the agreement between oil film and velocity gradient data is better the lower the speed and at longer distances from the jet exit. The wall gradient method of course works the best when the wall shear stress is low, since then the spatial resolution (in wall units) is the best. It is perhaps worth noting that the wall gradient data tend to be consistently lower than the oil film data. At higher levels of wall shear stress, this too is to be expected, since, at the lower spatial resolution (in wall units), the points measured closest to the wall are farther away from the wall as measured in wall units, where we expect the velocity gradient to be smaller.

The wall shear stress values from the momentum integral method are significantly higher than those obtained by the other two methods. This is, at least at first sight, surprising, since all three methods are theoretically exact, and should give the same results within the limits of the uncertainty in the basic measurements. The contributions by the various terms in the momentum equation was carefully examined, and the explanation cannot be found in the

uncertainties in the determination of these terms. The explanation thus must be either in the experimental set-up not being what we expect it to be, for example not being two-dimensional, or in the neglect of the terms not measured.

A hypothetical explanation might be offered by the $\overline{v^2}$ term. In the previously mentioned work, Johansson and Castillo,[1] it was found that the wall shear stress along a flat plate was very sensitive also to a minute pressure gradient. In that case the contribution to the wall shear stress from the $\overline{v^2}$ term was negligible, since this term reached appreciable values only close to the wall, where changes in the downstream directions are slow. In the wall-jet the situation seems to be reversed. The pressure gradient outside the wall jet is, in this case, zero, and should thus not contribute. On the other hand, the $\overline{v^2}$ term reaches large values in the outer part of the wall jet, where the changes in the downstream direction are much more rapid than close to the wall. This has the effect to lower the pressure close to the wall. Since the velocity level decreases downstream, it is expected that the pressure decrease across the wall jet decreases downstream, thus creating an adverse pressure gradient in a sizeable fraction of the wall jet, particularly close to the wall. Physically this means that the wall friction in the wall jet is lower than had not this pressure effect been present. Neglecting the $\overline{v^2}$ term thus means that we obtain a too high value of the wall shear stress.

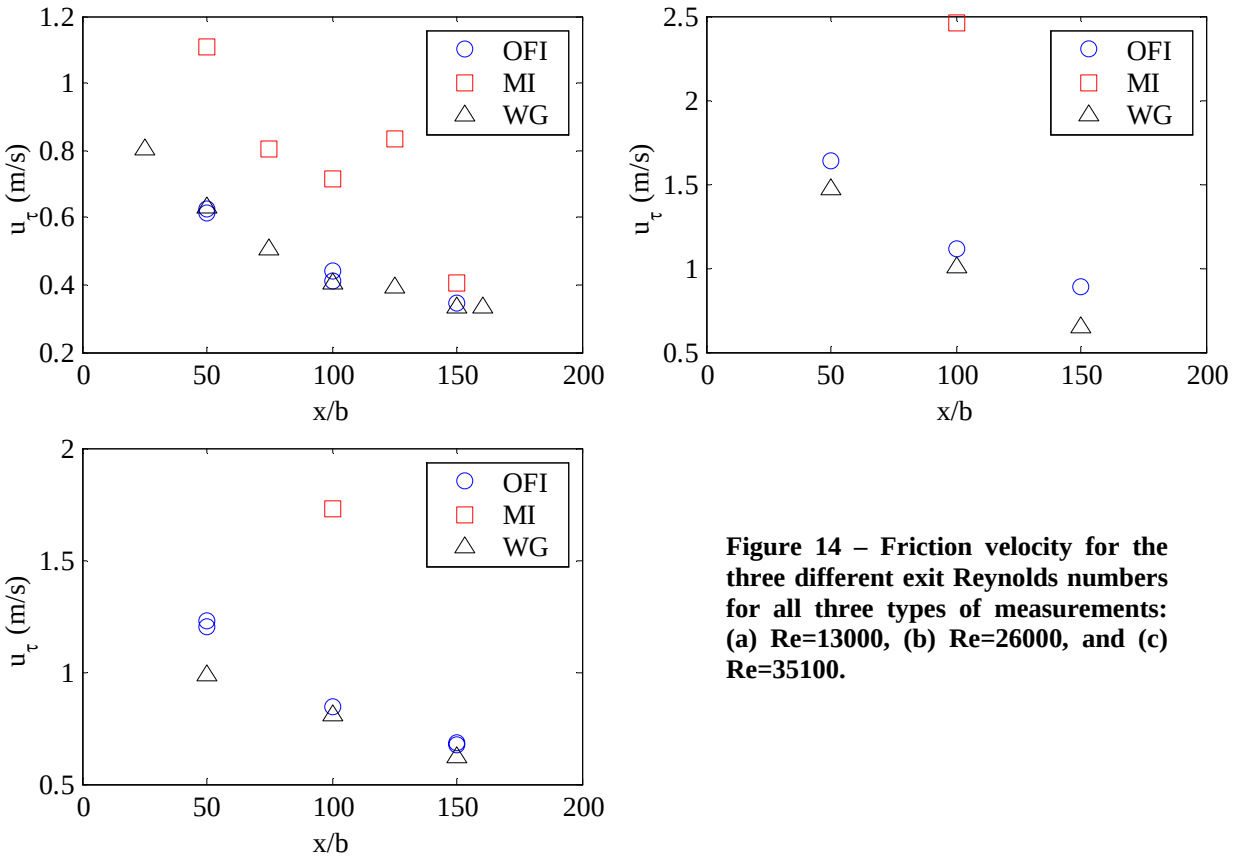

Figure 14 – Friction velocity for the three different exit Reynolds numbers for all three types of measurements: (a) Re=13000, (b) Re=26000, and (c) Re=35100.

V. Conclusion

Three methods of measuring the wall shear stress have been investigated, oil film interferometry, wall gradient method, and the momentum integral. In principle, all three methods are exact, but in their application here they yielded quite different results. The oil film method appears to give reliable measurements of wall shear stress at all levels of shear stress. However, the results show greater scatter than expected due to to surface imperfections and dust contamination. The results using oil-film method are consistent and show good agreement with the data from the wall gradient method at low shear stress levels. At higher shear stress levels, the data from the wall gradient method deviates from the oil film data in a way that is in correspondence with the effective decrease in resolving the

near-wall velocity profile. The momentum integral method needs further investigation before reliable conclusions can be made. At the present time the oil film method seems to be the most reliable of the three methods considered here.

There are several ways of improving the current measurements. Replacing the original wall jet surface with a glass surface will remove uncertainty associated with the imperfections in the Mylar film and is planned for the next phase of this comparison. Glass is an excellent surface due to its optical properties and its extremely flat surface. In addition to the current use of a tent to limit dust in the facility, the stilling chamer of the wall jet will be cleaned to remove any dust deposits. The wall gradient method can, as has been mentioned before, probably be improved by working at very low seeding levels. Still the method seems to be most useful at low values of the wall shear stress. The missing terms in the momentum integral method need to be evaluated to explain the differences in the wall shear stress measurements observed here.

Acknowledgments

This work was carried out while J. W. Naughton was a visiting professor at Chalmers University of Technology. The partial financial support of J. W. Naughton by the Turbulence Research Laboratory at Chalmers during his stay is appreciated.

References

[1]Johansson, T. and Castillo, L., "Near-Wall Measurements in Turbulent boundary Layers using Laser Doppler Anemometry," Proceedings of the, 2002 Joint US ASME-European Fluids Engineering Summer Conference July 14-18, 2002, Montreal, Canada. FEDSM2002-31070, 2002.

[2]Tanner, L. and Blows, L., "A Study of the Motion of Oil Films on Surfaces in Air Flow, with Application to the Measurement of Skin Friction," *Journal of Physics E: Scientific Instrumentation*, No. 3, 9 1976, pp. 194-202.

[3]Monson, D., Mateer, G., and Menter, F., "Boundary-Layer Transition and Global Skin Friction Measurement with an Oil-Fringe Imaging Technique," SAE Paper No. 932550, 1993.

[4]Mateer, G., Monson, D., and Menter, F., "Skin-Friction Measurements and Calculations on a Lifting Airfoil," *AIAA Journal*, Vol. 34, No. 2, 1996, pp. 231-236.

[5]Garrison, T. and Ackman, M., "Development of a Global Interferometer Skin-Friction Meter," *AIAA Journal*, Vol. 36, No. 1, 1998, pp. 62-68.

[6]Naughton, J. and Brown, J., "Surface Interferometric Skin-Friction Measurement Technique," AIAA Paper 96-2183, 1996.

[7]Naughton, J. W. and Sheplak, M., "Modern Developments in Shear Stress Measurement," *Progress in Aerospace Sciences*, Vol. 38, 2002, pp. 515-570.

[8]Squire, L., "The Motion of a Thin Oil Sheet Under the Boundary Layer on a Body," Flow Visualization in Wind Tunnels Using Indicators, AGARDograph 70, edited by R. Maltby, 1962, pp. 7-23.

[9]Brown, J. and Naughton, J., "The Thin Oil Film Equation," NASA-TM 1999-208767, NASA-Ames Research Center, March 1999.

[10]Naughton, J. W., Viken, S., and Greenblatt, D., "Skin Friction Measurements on the NASA Hump Model," *AIAA Journal*, Accepted for Publication, 2005.

[11]Cattafesta, III, L. N. and Moore, J. G., "Review and Application of Non-Topographic Photogrammetry to Quantitative Flow Visualization," AIAA Paper 96-2180, June 1996.

[12]Liu, T., Cattafesta, III, L. N., and Radetsky, R. H., "Photogrammetry Applied to Wind Tunnel Testing," *AIAA Journal*, Vol. 38, No. 6, June 2000, pp. 964-971.

[13]Decker, R. K., Naughton, J. W., and Jafari, F., "Automatic Fringe Detection for Oil Film Interferometric Skin-Friction Measurement," Proceedings of the 9th International Symposium on Flow Visualization, edited by I. Grant and G. Carlomagno, Paper 368, (on CD ROM, ISBN 0 9533991 1 7), 2000.

[14]Karlsson and Eriksson, private communication.